



**Providing Choice & Value**

Generic CT and MRI Contrast Agents



CONTACT REP

**AJNR**

This information is current as of July 21, 2025.

**Follow-up of Intracranial Aneurysms Treated by Flow Diverters: Evaluation of Parent Artery Patency Using 3D-T1 Gradient Recalled-Echo Imaging with 2-Point Dixon in Combination with 3D-TOF-MRA with Compressed Sensing**

J. Burel, E. Gerardin, M. Vannier, A. Curado, M. Verdalle-Cazes, N. Magne, M. Lefebvre and C. Papagiannaki

*AJNR Am J Neuroradiol* 2022, 43 (4) 554-559

doi: <https://doi.org/10.3174/ajnr.A7448>

<http://www.ajnr.org/content/43/4/554>

# Follow-up of Intracranial Aneurysms Treated by Flow Diverters: Evaluation of Parent Artery Patency Using 3D-T1 Gradient Recalled-Echo Imaging with 2-Point Dixon in Combination with 3D-TOF-MRA with Compressed Sensing

J. Burel, E. Gerardin, M. Vannier, A. Curado, M Verdalle-Cazes, N. Magne, M. Lefebvre, and C. Papagiannaki

## ABSTRACT

**BACKGROUND AND PURPOSE:** MRA assessment of parent artery patency after flow-diverter placement is complicated by imaging artifacts produced by these devices. The purpose of this study was to assess the accuracy of liver acquisition with volume acceleration-flex technique (LAVA-Flex) MRA in combination with 3D-TOF with HyperSense MRA for the evaluation of parent vessel status after intracranial flow-diverter placement.

**MATERIALS AND METHODS:** Fifty-six patients treated by flow diversion and followed with both DSA and 3T MRA between November 2020 and August 2021 were included. All patients were evaluated for parent artery patency using the same imaging protocol (DSA, noncontrast MRA including 3D-TOF with HyperSense and LAVA-Flex, and contrast-enhanced MRA, including time-resolved imaging of contrast kinetics MRA and delayed contrast-enhanced MRA).

**RESULTS:** With DSA as a criterion standard to evaluate the patency of the parent vessel, noncontrast MRA had a good specificity (0.83) and positive predictive value (0.65), better than contrast-enhanced MRA (0.55 and 0.41, respectively). Both had excellent sensitivity and negative predictive value: noncontrast MRA, 0.93 and 0.97, respectively; contrast-enhanced MRA, 0.93 and 0.96, respectively. Specificity and positive predictive value tended to be lower for patients treated with additional devices than for those treated with flow diverters exclusively and for patients treated with a specific type of flow diverter.

**CONCLUSIONS:** Noncontrast MRA can be used for noninvasive follow-up of intracranial aneurysms treated by flow diverters. The combined use of LAVA-Flex and 3D-TOF with HyperSense sequences allows monitoring the status of the parent artery and aneurysm occlusion.

**ABBREVIATIONS:** CE-MRA = contrast-enhanced MRA; FD = flow diverter; LAVA-Flex = liver acquisition with volume acceleration-flex technique; NC-MRA = noncontrast MRA; NPV = negative predictive value; PPV = positive predictive value; TRICKS = time-resolved imaging of contrast kinetics; VA = vertebral artery

Flow Diverters (FDs) were initially developed to treat wide-neck large and giant ICA aneurysms only amenable to surgical trap with or without a bypass or endovascular vessel sacrifice, but they have rapidly increased in use.<sup>1-4</sup> Due to the characteristics of these devices, a careful radiologic follow-up is required to assess the status of the aneurysmal occlusion and the patency of the parent artery.<sup>5</sup>

The rate of complete aneurysm occlusion after flow-diverter treatment varies among series, and it gradually increases with

time due to remodeling of the parent vessel.<sup>6,7</sup> Kallmes et al<sup>18</sup> performed a pooled analysis of 3 large studies, with a total of 1091 patients included. The complete occlusion rates were 75.0%, 85.5%, 93.4%, and 95.2% at 6 months and 1, 3, and 5 years, respectively; the overall retreatment rate was low, 3.0%. These retreatments almost exclusively concern aneurysms that persist despite FD placement, with aneurysmal recanalization being exceptional.<sup>9,10</sup> Thus, an aneurysm treated by a flow diverter whose complete occlusion has been proved is generally considered permanently occluded.<sup>8,11-14</sup> Hence, once this occlusion has been obtained, whether it is observed by DSA or MRA (with or without injection of contrast media),<sup>15-18</sup> long-term parent artery patency and parenchymal complications are the essential elements to monitor, preferably with noninvasive imaging.

MR imaging is the criterion standard for evaluating potential ischemic and hemorrhagic complications after FD placement and

Received November 5, 2021; accepted after revision January 3, 2022.

From the Departments of Radiology (J.B., E.G., A.C., M.V.-C., N.M., M.L., C.P.) and Biostatistics (M.V.), Rouen University Hospital, Rouen, Normandie, France.

Please address correspondence to Julien Burel, MD, Rouen University Hospital, 37 Boulevard Gambetta, Rouen 76031; e-mail: julien.burel@chu-rouen.fr

Indicates article with online supplemental data.

<http://dx.doi.org/10.3174/ajnr.A7448>

can also identify aneurysm enlargement, aneurysm wall enhancement, and perianeurysmal edema.<sup>19</sup> DSA is the criterion standard for the evaluation of aneurysm occlusion, but 3D-TOF-MRA and CE-MRA have excellent diagnostic accuracy for the aneurysm remnant and can be used in follow-up.<sup>15-18,20</sup> DSA is also the criterion standard for the evaluation of parent vessel patency after treatment by a FD, due to its unsurpassed spatial resolution and its insusceptibility to metal artifacts. However, DSA is invasive and has potential complications, either of the puncture site or neurologic.<sup>21</sup> Regarding the evaluation of parent artery patency, the performance of conventional MRA sequences was initially considered insufficient.<sup>15,16</sup> Recently, Oishi et al<sup>5</sup> and Shao et al<sup>22</sup> evaluated the performance of Silent MRA (GE Healthcare) and 3D-T1 sampling perfection with application-optimized contrasts by using different flip angle evolution (SPACE sequence; Siemens), respectively, to assess the parent artery status after FD placement. The results were good, but the sequences used took several minutes (12 minutes 13 seconds and 8 minutes 29 seconds, respectively) to acquire and were consequently more susceptible to motion artifacts due to swallowing or gross body movement. In addition, the 3D-T1 SPACE sequence could not be used to study aneurysmal occlusion; therefore, an additional 3D-TOF sequence was necessary.

The liver acquisition with volume acceleration-flex technique (LAVA-Flex) sequence, initially developed for liver imaging, is now used in other imaging fields. Regarding neurovascular imaging, Irie et al<sup>23</sup> concluded that LAVA-Flex MRA could provide information similar to TOF-MRA for assessing the cervical carotid bifurcation while reducing scan time by one-fifth. To our knowledge, the use of this sequence for the analysis of intracranial FDs or any type of intracranial stent has not been evaluated. The purpose of this study was to assess the accuracy of LAVA-Flex MRA in combination with 3D-TOF with HyperSense MRA (GE Healthcare) for the evaluation of parent artery patency after intracranial FD placement.

## MATERIALS AND METHODS

### Patient and FD Characteristics

All patients treated with FDs at our institution and followed with both MRA and DSA were prospectively included in a data base. Patients who underwent both DSA and 3T MRA within a maximum interval of 4 weeks, between November 2020 and August 2021, were included. Exclusion criteria were patients with a contraindication to MR imaging, patients who refused to undergo examinations (MR imaging or DSA), and those who did not undergo one or more of the 4 MRA sequences listed below. The Online Supplemental Data summarize the main technical characteristics of the devices used and evaluated in this study.

### DSA Technique

Intra-arterial DSA was performed with a biplane angiographic system (Allura Xper; Philips Healthcare). By means of transfemoral 4F catheterization, selective injections of the ICA or vertebral artery (VA) were performed according to the FD location. Standard anterior-posterior and lateral projections were routinely acquired. For the ICA, 8 mL of nonionic contrast agent (iodixanol, 320-mg iodine/mL, Visipaque 320; GE Healthcare) were

injected with a velocity of 4 mL/s. For the VA, 6 mL was injected with a velocity of 3 mL/s. Rotational 3D angiography and selected oblique projections were performed for additional confirmation of findings. All acquired DSA images were converted to internationally compatible DICOM files; then the converted files were transferred to our server through a PACS.

### MRA Technique

MRA examinations were performed on a 3T MR imaging system (Discovery MR750; GE Healthcare) using a 32-channel head coil. MR imaging protocol included axial FLAIR, 2 noncontrast MRA (NC-MRA) sequences (LAVA-Flex and 3D-TOF with HyperSense), and 2 contrast-enhanced MRA (CE-MRA) sequences (time-resolved imaging of contrast kinetics [TRICKS] and a delayed 3D spoiled gradient-echo sequence). TRICKS MRA was performed after the injection of a gadolinium-based contrast agent (gadobutrol, Gadovist; Bayer HealthCare) prescribed at 0.1-mmol/kg and 1-mL/s injection rates, followed immediately by 20–30 mL of normal saline flush at 1 mL/s. An MR fluoroscopic triggering technique was used. The temporal resolution was 1.7 s/frame. The delayed CE-MRA sequence was initiated immediately after acquisition of the TRICKS MRA without application of additional contrast media. Scan parameters of NC-MRA sequences and CE-MRA sequences are summarized in the Online Supplemental Data.

### Image Analysis

Studies from all patients were placed in an anonymized folder on the PACS, with NC-MRA (LAVA-Flex MRA and 3D-TOF-MRA with HyperSense), CE-MRA (TRICKS MRA and delayed CE-MRA), and DSA studies forming 3 anonymized folders. The entire original acquired data set, including both source images (mask, subtracted, and unsubtracted images) and standard reformats (MIP and MPR) for each technique, was made available for review when evaluating that technique. LAVA-Flex MRA and 3D-TOF-MRA with HyperSense were evaluated together to form the NC-MRA evaluation of parent artery patency, and TRICKS MRA and delayed CE-MRA were evaluated together to form the CE-MRA evaluation of parent artery patency. NC-MRA, CE-MRA, and DSA were evaluated separately without knowledge of the MRA or DSA examination results, by 1 interventional neuroradiologist and 1 diagnostic neuroradiologist (both MD-PhD, with >15 years' experience). The location of the FDs to be evaluated was provided to the readers. In case of disagreement, consensus was found between the 2 radiologists.

The patency status of the parent artery was evaluated as no change in the parent artery diameter (patent), focal or diffuse narrowing of the parent artery (stenosis), or parent artery occlusion. A simplified 2-grade scale was used to assess the patency of the parent artery, in which the parent artery was classified as normal or pathologic (stenosis or occlusion). An example of each technique for 1 patient is shown in the Online Supplemental Data.

### Statistical Analysis

Quantitative variables are reported as mean (SD) and median (range), while qualitative variables are reported as number and percentage. Interobserver and intermodality agreement was calculated using the Cohen  $\kappa$ . The interpretation of  $\kappa$  was as follows:  $\kappa < 0$ ,

**Table 1: Evaluation of parent artery patency (n = 56)**

	NC-MRA	CE-MRA	DSA
Three-grade scale			
Patent	36 (64.3%)	24 (42.9%)	42 (75.0%)
Stenosis	19 (33.9%)	31 (55.4%)	13 (23.2%)
Occlusion	1 (1.8%)	1 (1.8%)	1 (1.8%)
Simplified 2-grade scale			
Patent	36 (64.3%)	24 (42.9%)	42 (75.0%)
Stenosis or occlusion	20 (35.7%)	32 (57.1%)	14 (25.0%)

**Table 2: Four-fold table of NC-MRA using consensus evaluation for NC-MRA and DSA**

	Consensus Evaluation for DSA	
	Pathologic (Stenosis or Occlusion)	Normal (Patent)
Consensus Evaluation for NC-MRA		
Pathologic (stenosis or occlusion)	13	7
Normal (patent)	1	35

no agreement;  $\kappa = 0-0.19$ , poor agreement;  $\kappa = 0.20-0.39$ , fair agreement;  $\kappa = 0.40-0.59$ , moderate agreement;  $\kappa = 0.60-0.79$ , substantial agreement; and  $\kappa = 0.80-1.00$ , almost perfect agreement.<sup>24</sup> Contingency tables were used to summarize the relationships: NC-MRA versus DSA and CE-MRA versus DSA, using the consensus evaluation. With DSA as a criterion standard to evaluate the patency of the parent artery, the sensitivity, specificity, negative predictive value (NPV), and positive predictive value (PPV) of NC-MRA and CE-MRA were calculated for the whole population, using the consensus evaluation with corresponding 95% confidence intervals. For NC-MRA, these calculations were also made for each separate device, for patients treated with FDs exclusively and those treated with additional devices (coils, Woven EndoBridge [WEB; MicroVention], surgical clips). Comparison between possible receiver operating characteristic curves was not performed due to relatively small samples. All analyses were performed using SAS software, Version 9.4 (SAS Institute).

## RESULTS

Fifty-six patients were included, 44 women (78.6%) and 12 men (21.4%), with a mean age of 57.8 (SD, 10.2) years (range, 25–79 years). Fifty-two of the 56 patients (92.9%) were treated with 1 FD; and 4 patients (7.1%), with 2 partially overlapping FDs in the same treatment. Twenty-eight of the 56 patients (50.0%) were treated with a Pipeline Shield FD (Medtronic); 19 (33.9%), with a Surpass Evolve FD (Stryker Neurovascular); and 9 (16.1%), with a Silk Vista Baby FD (Balt Extrusion). Twenty-two patients (39.3%) were treated with FDs exclusively; 32 (57.1%), with additional coils; 1, with a prior surgical clip (1.8%); and 1 (1.8%), with a WEB device. The anatomic distribution of FDs was as follows: intracranial ICA and/or M1 segment of the MCA ( $n = 39$ ); intracranial VA, basilar artery, and/or the P1 segment of the posterior cerebral artery ( $n = 7$ ); anterior communicating artery complex ( $n = 6$ ); and more distal vessels ( $n = 4$ ).

When we evaluated the status of the parent artery, interobserver agreement was 0.66 for NC-MRA, 0.67 for CE-MRA, and

**Table 3: Four-fold table of CE-MRA using consensus evaluation for CE-MRA and DSA**

	Consensus Evaluation for DSA	
	Pathologic (Stenosis or Occlusion)	Normal (Patent)
Consensus Evaluation for CE-MRA		
Pathologic (stenosis or occlusion)	13	19
Normal (patent)	1	23

1 for DSA. By means of the simplified 2-grade scale,  $\kappa$  was 0.65 for NC-MRA, 0.69 for CE-MRA, and 1 for DSA.

Table 1 shows the results of the assessment of parent artery patency with NC-MRA, CE-MRA, and DSA. Only 1 parent artery classified as patent on NC-MRA was classified as stenosis on DSA due to intimal hyperplasia (ie, 1 false-negative). Among the arteries classified as stenosis or occlusion on NC-MRA ( $n = 20$ ), 7 were patent on DSA (ie, 7 false-positives). There were 35 true-negatives and 13 true-positives. By means of CE-MRA, 1 parent artery classified as patent was classified as stenosis on DSA (ie, 1 false-negative, which was the same for NC-MRA). Among the arteries classified as stenosis or occlusion on CE-MRA ( $n = 32$ ), 19 were patent on DSA (ie, 19 false-positives). There were 23 true-negatives and 13 true-positives. Tables 2 and 3 present the corresponding 4-fold tables of these results.

By means of the 3-grade scale, intermodality agreement was 0.67 for NC-MRA/DSA and 0.35 for CE-MRA/DSA. With the simplified 2-grade scale,  $\kappa$  was 0.67 for NC-MRA/DSA and 0.33 for CE-MRA/DSA.

NC-MRA had a good specificity (0.83; 95% CI, 0.69–0.93) and PPV (0.65; 95% CI, 0.41–0.85), better than CE-MRA (0.55; 95% CI, 0.39–0.70; and 0.41; 95% CI, 0.24–0.59, respectively). Both had excellent sensitivity and NPV: 0.93; 95% CI, 0.66–1.00; and 0.97; 95% CI, 0.85–1.00, respectively, for NC-MRA and 0.93; 95% CI, 0.66–1.00; and 0.96; 95% CI, 0.79–1.00, respectively, for CE-MRA. Sensitivity, specificity, NPV, and PPV of NC-MRA for each separate device for patients treated with FD exclusively and those treated with an additional device are shown in Table 4.

## DISCUSSION

Currently, 3D-TOF-MRA is the most frequently used noninvasive follow-up method for intracranial aneurysms treated using endovascular techniques.<sup>20</sup> However, for patients who underwent flow diversion, the magnetic and radiofrequency shielding causes a signal loss in the stent implantation area and often manifests as a false in-stent stenosis or interruption and, consequently, has poor specificity and PPV. To reduce these metallic artifacts, Oishi et al<sup>5</sup> and Shao et al<sup>22</sup> used, respectively, Silent MRA and 3D-T1 SPACE to assess the parent artery status. Regarding the patency of the stented arteries after FD treatment, these sequences were more accurate compared with 3D-TOF-MRA, but they were time-consuming and, consequently, more susceptible to motion artifacts. To reduce the duration of the sequences and reduce the possible motion artifacts and the total duration of the MR imaging examination procedure, we have optimized 2 sequences, which we use together: a 3D-TOF sequence with HyperSense and

**Table 4: Diagnostic accuracies for parent artery patency of NC-MRA for each separate device, for patients treated with FD exclusively and those treated with additional device**

	Pipeline Shield (n = 28)	Surpass Evolve (n = 19)	Silk Vista Baby (n = 9)	FD Exclusively (n = 22)	Additional Device (n = 34)
Specificity (95% CI)	0.96 (0.78–1.00)	0.57 (0.29–0.82)	1 (0.48–1.00)	0.87 (0.60–0.98)	0.81 (0.62–0.94)
PPV (95% CI)	0.80 (0.28–0.99)	0.45 (0.17–0.77)	1 (0.40–1.00)	0.78 (0.40–0.97)	0.55 (0.23–0.83)
Sensitivity (95% CI)	0.80 (0.28–0.99)	1 (0.48–1.00)	1 (0.40–1.00)	1 (0.59–1.00)	0.86 (0.42–1.00)
NPV (95% CI)	0.96 (0.78–1.00)	1 (0.63–1.00)	1 (0.48–1.00)	1 (0.75–1.00)	0.96 (0.78–1.00)

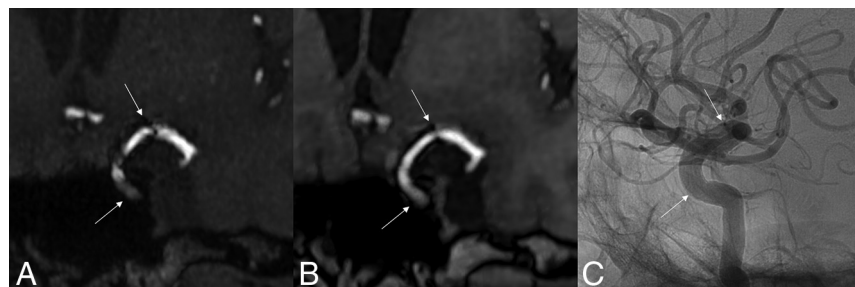


**FIG 1.** 3D-TOF with HyperSense MRA (A), LAVA-Flex MRA (B), and DSA (C) of a 61-year-old woman treated with a 4 × 25 Surpass Evolve FD located from the left ICA to the left MCA. There is a significant reduction in metal artifacts on the LAVA-Flex (OutPhase) sequence, which shows the absence of in-stent stenosis, confirmed by DSA. Note that there is not exactly the same projection between MRA and DSA. White arrows indicate the proximal and distal ends of the FDs.

a LAVA-Flex sequence, both without injection of a contrast agent. The LAVA-Flex sequence allows better study of the flow inside the stent, whereas the 3D-TOF sequence remains necessary to study aneurysmal occlusion because the LAVA-Flex sequence has not proved its effectiveness for this purpose.

Apart from increasing the signal-to-noise ratio, especially intravascular, the compressed sensing technique HyperSense allows a substantial reduction in the acquisition time of the 3D-TOF sequence. Ours had a total acquisition time of 2 minutes 59 seconds. This sequence can also be used to evaluate aneurysmal occlusion, analyze other arteries, but also, when artifacts are low, to evaluate the patency of the parent artery. The LAVA-Flex sequence allows, with a particularly short acquisition time of 1 minute 57 seconds, a 3D-T1-weighted sequence that is less sensitive to metallic artifacts, in particular on the out of phase sequence due to a shorter TE (Fig 1), with, however, a weaker intravascular signal due to an entry section phenomenon less marked than the 3D-TOF with HyperSense sequence. This can be explained by the shorter TR of the LAVA-Flex sequence compared with the 3D-TOF sequence; however, this short TR results in a remarkably decreased acquisition time, without hindering the in-stent flow analysis. MIP reformats of LAVA-Flex MRA are useful to evaluate the caliber of the parent vessel but must always be analyzed in conjunction with the native sections because the selection of the most intense voxels by the MIP algorithm hinders the visualization of the stent, whose signal is low. The total acquisition time for these 2 sequences was, therefore, 4 minutes 56 seconds, more than 2 times shorter than Silent MRA or 3D-T1 SPACE combined with 3D-TOF.

In this study, the joint use of 3D-TOF with HyperSense MRA and LAVA-Flex MRA allowed us to obtain a NC-MRA specificity of 0.83 (95% CI, 0.69–0.93) and a PPV of 0.65 (95% CI, 0.41–0.85) (Fig 2), which were better than those of CE-MRA (0.55; 95% CI, 0.39–

0.70; and 0.41; 95% CI, 0.24–0.59, respectively) in the evaluation of the parent artery patency. This result can be explained by an analysis of the TRICKS MRA sequence generally using background-subtracted volumes, which do not permit stent visualization, as well as the use of a delayed-MRA sequence, and not an arterial CE-MRA sequence. Finally, the absence of a contrast-enhanced 3D-T1-weighted sequence can also partially explain these results. With NC-MRA and CE-MRA, we had only 1 false-negative result, which can probably be explained by the delay between MR imaging and arteriography, 4 weeks for this patient, who had

stopped the dual antiplatelet therapy on his own after the MR imaging examination, 3 months after FD placement at the M1–M2 junction. Thus, the in-stent stenosis could have developed in the meantime. The sensitivity and NPV remained excellent for NC-MRA (0.93; 95% CI, 0.66–1.00; and 0.97; 95% CI, 0.85–1.00, respectively) and CE-MRA (0.93; 95% CI, 0.66–1.00; and 0.96; 95% CI, 0.79–1.00, respectively).

The specificity and PPV tended to be lower for Pipeline Shield FDs and even lower for Surpass Evolve FDs, probably due to more pronounced metallic artifacts (Fig 3). Unlike the criterion standard DSA, MRA is susceptible to the dissimilarities between flow diverters. Halitan et al<sup>15</sup> suggested that the key factor was the alloy used for the construction of the FDs, with nitinol-based devices being responsible for fewer metallic artifacts. While we agree that this factor influences the extent of artifacts, the marked difference between the artifacts created by Pipeline Shield FDs and Surpass Evolve FDs, which are both cobalt-chromium devices, suggests that other important factors were probably involved, such as the number of wires composing the FD combined with the thickness of the wire. Indeed, Surpass Evolve FDs are made of 64 wires (except for 2.5 mm diameter FD), while Pipeline Shield FDs are made of 48 wires, with an equivalent wire thickness (~28 and ~30 μm, respectively). In addition, the tungsten used in combination with platinum for the visibility of cobalt-chromium devices used in this study (while nitinol devices used only platinum) may also play a role.

It is important to keep in mind the shortcomings of each FD in MR imaging when interpreting the parent artery patency, so as not to erroneously conclude in-stent stenosis. Specificity and PPV tended to be lower for patients treated with additional devices than for those treated with FDs exclusively, an outcome expected due to the additional artifacts created by coils, the WEB, or surgical clips. Indeed, these artifacts can appear as false stenosis (ie, false-positives),

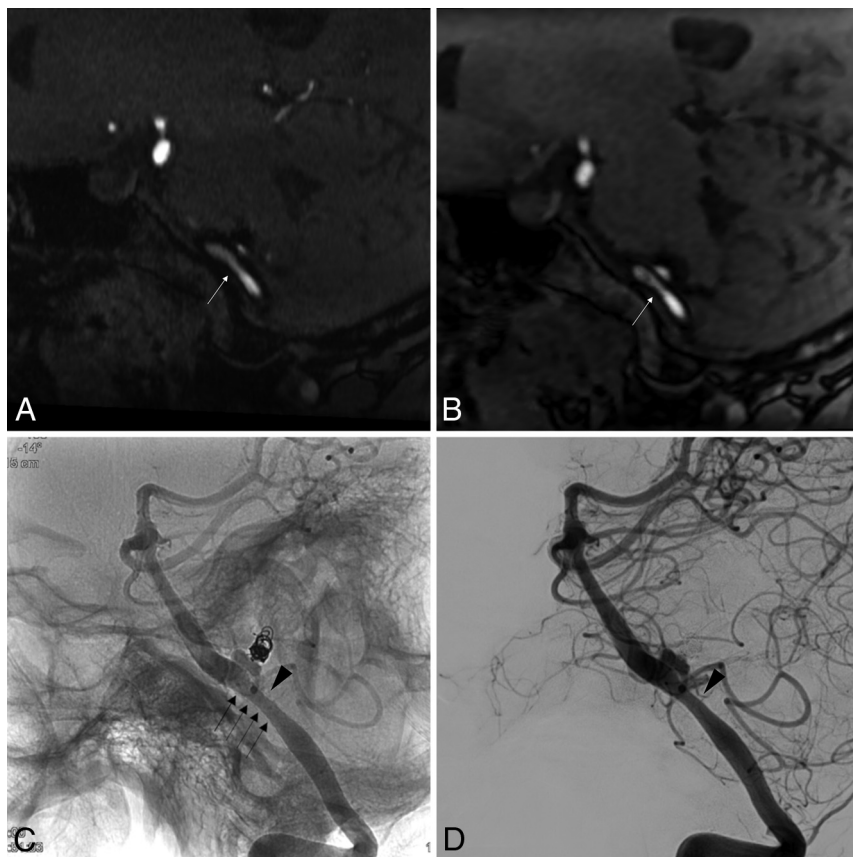


**FIG 2.** In-stent stenosis in a 50-year-old woman treated with a  $5 \times 15$  Surpass Evolve FD placed in the left VA. This was a complementary embolization of a left PICA aneurysm, initially revealed by a subarachnoid hemorrhage 10 years earlier and treated by coiling at that time. 3D-TOF with HyperSense MRA (A) and LAVA-Flex MRA (Outphase) (B) demonstrates moderate in-stent stenosis (white arrows) predominating a few millimeters upstream of the neck of the still patent aneurysm, 6 months after placement of the FD. Confirmation of a moderate in-stent stenosis (black arrowhead) on angiography without (C) and with (D) digital subtraction. The black arrows show the limits of the FD metallic mesh.

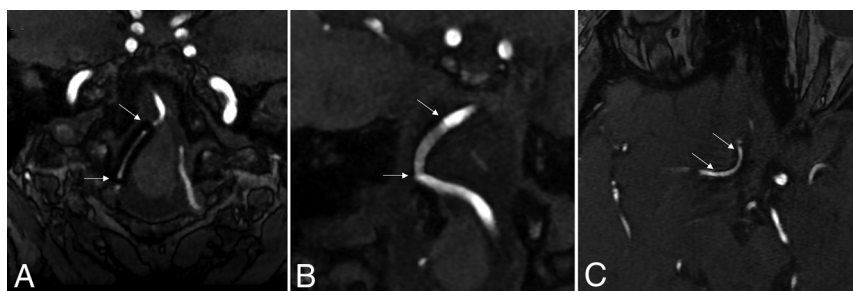


**FIG 3.** 3D-TOF with HyperSense MRA comparison of artifacts created by the 3 types of FDs used in our study. A, A 68-year-old woman treated with a Surpass Evolve FD ( $3.25 \times 17$  mm) located in the right VA. B, A 61-year-old woman treated with a Pipeline Shield FD ( $3.5 \times 18$  mm) located from the left VA to the basilar artery. C, A 52-year-old woman treated with a Silk Vista Baby FD ( $2.5 \times 20$  mm) located in the right anterior cerebral artery (A1–A2). The extent of the metallic artifacts is large for the Surpass Evolve FD, small for the Pipeline Shield FD, and minimal for the Silk Vista Baby FD. White arrows indicate the proximal and distal ends of the FDs.

thus reducing specificity and PPV. MR imaging is essential for the evaluation of potential ischemic and hemorrhagic complications after FD placement and is a relatively reliable screening test for in-

stant stenosis because of its excellent sensitivity and NPV. However, DSA remains the criterion standard in parent artery patency evaluation, especially when additional material like coils or surgical clips is used. It, thus, appears useful to systematically perform NC-MRA sequences in addition to classic parenchymal sequences to evaluate in-stent flow. Ideally, an initial concomitant DSA control would indicate any false-positive or false-negative results, which could serve as reference in the long-term follow-up of intracranial stent evaluation with NC-MRA.

Our study has some limitations: First, the small number of patients ( $n = 56$ ) included. However, this number is comparable with that in the other 2 main studies focused on the analysis of the patency of the parent artery (40 for Shao et al<sup>22</sup> and 78 for Oishi et al<sup>5</sup>). Besides, the sample size for each kind of FD is small, possibly introducing systematic error. Second, MR imaging and DSA were not systematically performed on the same day, with a maximum interval of 4 weeks and, therefore, may not reflect the exact same conditions concerning parent vessel status. Third, CTA was not evaluated in our study, notably for patients treated with FDs exclusively for whom it could be a valid option. Although it shares the risks of iodinated contrast media and ionizing radiation of DSA, it is a noninvasive examination that does not share the potential risks of puncture site and neurologic complications. Fourth, interobserver agreement ranged from 0.6 to 0.79 for the NC-MRA and CE-MRA, corresponding to “substantial agreement” and not “almost perfect agreement.”<sup>24</sup> These differences mainly concerned the analysis of Surpass Evolve FDs, which produce more pronounced metallic artifacts than the other FDs studied, thus making interpretation more difficult, especially in the presence of additional material like coils and clips.

## CONCLUSIONS

NC-MRA can be used for noninvasive especially long-term follow-up of intracranial aneurysms treated by FDs. The combined use of LAVA-Flex and 3D-TOF with HyperSense sequences is accurate compared with DSA and allows

monitoring the status of the parent artery and aneurysmal occlusion. These two sequences could be useful tools, especially in the long- and very-long-term follow-up of these devices. The total acquisition time with these 2 sequences is reduced by at least half compared with Silent MRA or 3D-T1 SPACE combined with 3D-TOF. Specificity and PPV depend on the type of FD and whether patients are treated with additional devices (coils, intrasaccular flow disruptors, surgical clips).

**Disclosure forms** provided by the authors are available with the full text and PDF of this article at [www.ajnr.org](http://www.ajnr.org).

## REFERENCES

1. Nelson PK, Lylyk P, Szikora I, et al. **The Pipeline Embolization Device for the intracranial treatment of aneurysms trial.** *AJNR Am J Neuroradiol* 2011;32:34–40 [CrossRef Medline](#)
2. Kallmes DF, Hanel R, Lopes D, et al. **International retrospective study of the Pipeline Embolization Device: a multicenter aneurysm treatment study.** *AJNR Am J Neuroradiol* 2015;36:108–15 [CrossRef Medline](#)
3. Brinjikji W, Murad MH, Lanzino G, et al. **Endovascular treatment of intracranial aneurysms with flow diverters: a meta-analysis.** *Stroke* 2013;44:442–47 [CrossRef Medline](#)
4. Dandapat S, Mendez-Ruiz A, Martínez-Galdámez M, et al. **Review of current intracranial aneurysm flow diversion technology and clinical use.** *J Neurointerv Surg* 2021;13:54–62 [CrossRef Medline](#)
5. Oishi H, Fujii T, Suzuki M, et al. **Usefulness of silent MR angiography for intracranial aneurysms treated with a flow-diverter device.** *AJNR Am J Neuroradiol* 2019;40:808–14 [CrossRef Medline](#)
6. O'Kelly CJ, Spears J, Chow M, et al. **Canadian experience with the Pipeline Embolization Device for repair of unruptured intracranial aneurysms.** *AJNR Am J Neuroradiol* 2013;34:381–87 [CrossRef Medline](#)
7. Briganti F, Napoli M, Leone G, et al. **Treatment of intracranial aneurysms by flow diverter devices: long-term results from a single center.** *Eur J Radiol* 2014;83:1683–90 [CrossRef Medline](#)
8. Kallmes DF, Brinjikji W, Cekirge S, et al. **Safety and efficacy of the Pipeline embolization device for treatment of intracranial aneurysms: a pooled analysis of 3 large studies.** *J Neurosurg* 2017;127:775–80 [CrossRef Medline](#)
9. Zhang X, Lv N, Wang C, et al. **Late recurrence of a completely occluded large intracranial aneurysm treated with a Tubridge flow diverter.** *Neurointerv Surg* 2017;9:e6 [CrossRef Medline](#)
10. Trivelato FP, Ulhoa AC, Rezende MT, et al. **Recurrence of a totally occluded aneurysm after treatment with a Pipeline Embolization Device.** *BMJ Case Rep* 2018;2018:bcr-2018013842 [CrossRef Medline](#)
11. Soize S, Gawlitza M, Raoult H, et al. **Imaging follow-up of intracranial aneurysms treated by endovascular means: why, when, and how?** *Stroke* 2016;47:1407–12 [CrossRef Medline](#)
12. Gupta R, Ogilvy CS, Moore JM, et al. **Proposal of a follow-up imaging strategy following Pipeline flow diversion treatment of intracranial aneurysms.** *J Neurosurg* 2018;131:32–39 [CrossRef Medline](#)
13. Becske T, Brinjikji W, Potts MB, et al. **Long-term clinical and angiographic outcomes following Pipeline Embolization Device treatment of complex internal carotid artery aneurysms: five-year Results of the Pipeline for Uncoilable or Failed Aneurysms Trial.** *Neurosurgery* 2017;80:40–48 [CrossRef Medline](#)
14. Deutschmann HA, Wehrschuetz M, Augustin M, et al. **Long-term follow-up after treatment of intracranial aneurysms with the Pipeline Embolization Device: results from a single center.** *AJNR Am J Neuroradiol* 2012;33:481–86 [CrossRef Medline](#)
15. Halitcan B, Bige S, Sinan B, et al. **The implications of magnetic resonance angiography artifacts caused by different types of intracranial flow diverters.** *J Cardiovasc Magn Reson* 2021;23:69 [CrossRef Medline](#)
16. Attali J, Benaissa A, Soize S, et al. **Follow-up of intracranial aneurysms treated by flow diverter: comparison of three-dimensional time-of-flight MR angiography (3D-TOF-MRA) and contrast-enhanced MR angiography (CE-MRA) sequences with digital subtraction angiography as the gold standard.** *J Neurointerv Surg* 2016;8:81–86 [CrossRef Medline](#)
17. Boddu SR, Tong FC, Dehkharghani S, et al. **Contrast-enhanced time-resolved MRA for follow-up of intracranial aneurysms treated with the Pipeline Embolization Device.** *AJNR Am J Neuroradiol* 2014;35:2112–18 [CrossRef Medline](#)
18. Patzig M, Forbrig R, Ertl L, et al. **Intracranial aneurysms treated by flow-diverting stents: long-term follow-up with contrast-enhanced magnetic resonance angiography.** *Cardiovasc Intervent Radiol* 2017;40:1713–22 [CrossRef Medline](#)
19. McGuinness BJ, Memon S, Hope JK. **Prospective study of early MRI appearances following flow-diverting stent placement for intracranial aneurysms.** *AJNR Am J Neuroradiol* 2015;36:943–48 [CrossRef Medline](#)
20. Ahmed SU, Mocco J, Zhang X, et al. **MRA versus DSA for the follow-up imaging of intracranial aneurysms treated using endovascular techniques: a meta-analysis.** *J Neurointerv Surg* 2019;11:1009–14 [CrossRef Medline](#)
21. Kaufmann TJ, Huston J, Mandrekar JN, et al. **Complications of diagnostic cerebral angiography: evaluation of 19,826 consecutive patients.** *Radiology* 2007;243:812–19 [CrossRef Medline](#)
22. Shao Q, Wu Q, Li Q, et al. **Usefulness of 3D T1-SPACE in combination with 3D-TOF MRA for follow-up evaluation of intracranial aneurysms treated with Pipeline Embolization Devices.** *Front Neurol* 2020;11:542493 [CrossRef Medline](#)
23. Irie R, Amemiya S, Ueyama T, et al. **Accelerated acquisition of carotid MR angiography using 3D gradient-echo imaging with two-point Dixon.** *Neuroradiology* 2020;62:1345–49 [CrossRef Medline](#)
24. Landis JR, Koch GG. **The measurement of observer agreement for categorical data.** *Biometrics* 1977;33:159–74 [CrossRef Medline](#)